Journal of Materials Chemistry C

Materials for optical and electronic devices

www.rsc.org/MaterialsC

Volume 1 | Number 29 | 7 August 2013 | Pages 4399–4506

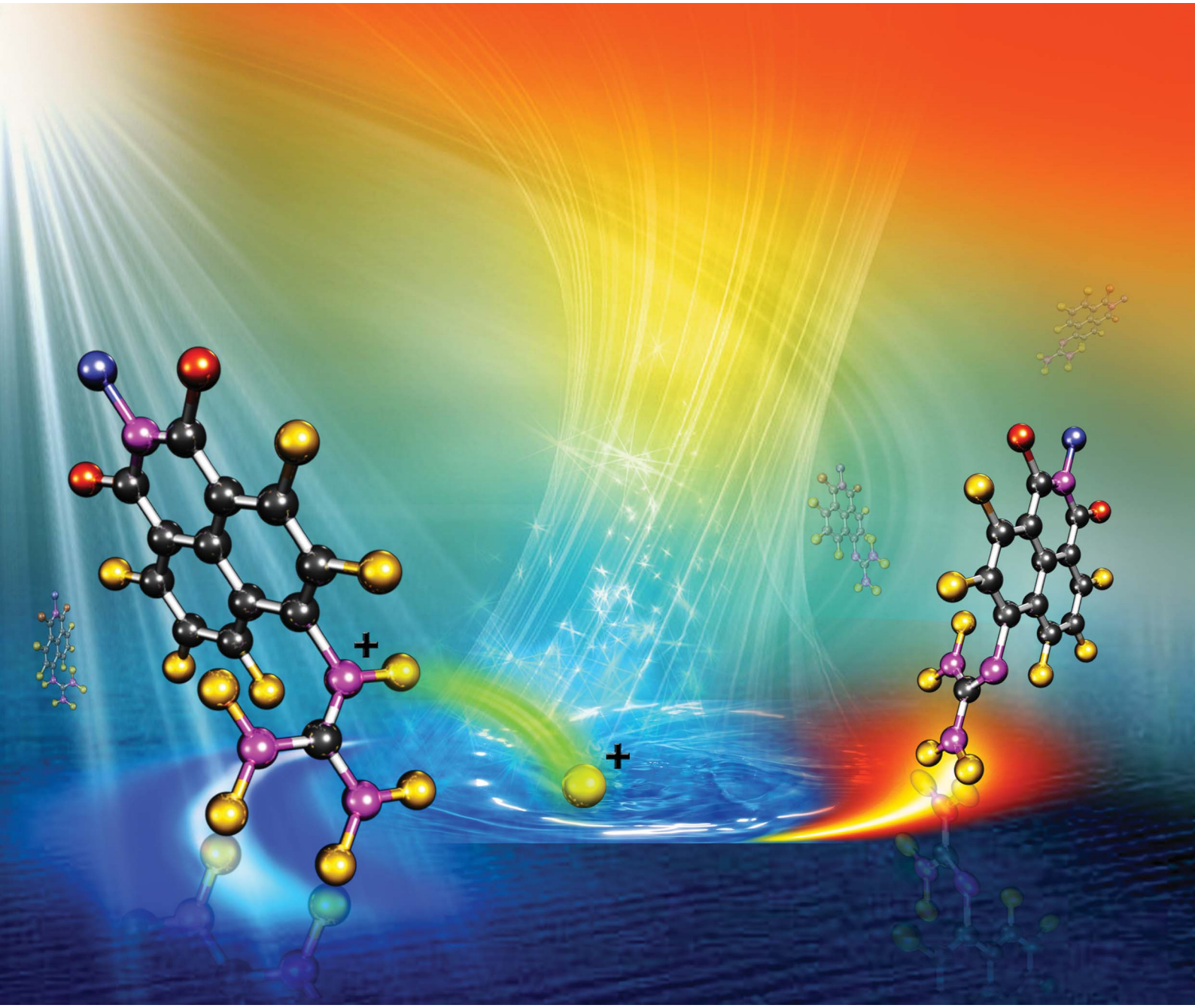

ISSN 2050-7526

RSC Publishing

PAPER

Dihua Shangguan *et al.*

A guanidine derivative of naphthalimide with excited-state deprotonation coupled intramolecular charge transfer properties and its application

2050-7526(2013)1:29;1-A

Journal of Materials Chemistry C

RSC Publishing

PAPER

View Article Online
View Journal | View Issue

Cite this: J. Mater. Chem. C, 2013, 1, 4427

A guanidine derivative of naphthalimide with excited-state deprotonation coupled intramolecular charge transfer properties and its application†

Jin Zhou,[ac] Huiying Liu,[b] Bing Jin,[ac] Xiangjun Liu,[a] Hongbing Fu[b] and Dihua Shangguan*[a]

Received 7th May 2013
Accepted 30th May 2013

DOI: 10.1039/c3tc30853g

www.rsc.org/MaterialsC

A new fluorophore based on guanidine substituted 1,8-naphthalimide was synthesized and characterized. In aqueous solution, the guanidine group undergoes deprotonation/protonation with a pK_a of ~8.5 in the ground-state and ~0.9 in the excited-state. The emission of its protonated and deprotonated forms exhibits a large Stokes shift (Ex/Em: 350/460 nm and 400/580 nm) due to the excited-state intramolecular charge transfer (ICT) process. The protonated form of this fluorophore exhibits dual fluorescence emission (Em: 460 and 580 nm; Ex: 350 nm) that is contributed to by an excited-state deprotonation coupled ICT process. The emission properties of this fluorophore are strongly dependent on the solvent environment, which make it possible to tune the luminescence of the materials made using this fluorophore. The absorption and emission spectra of this fluorophore respond to fluoride ions ratiometrically, showing the potential application as a fluoride ion sensor.

Introduction

Electron transfer and proton transfer are the most fundamental chemical reactions that play important roles in numerous chemical and biological processes. They are also the basis of different signaling mechanisms of various optical probes, such as, photoinduced electron transfer, metal–ligand charge transfer, twisted intramolecular charge transfer, electronic energy transfer, intramolecular charge transfer (ICT) and excited-state proton transfer (ESPT).[1] Recently, organic molecules with ESPT have received considerable attention because of their wide range of applications in laser materials,[2] photostabilizers,[3] optical sensors,[1c,4] energy storage systems[5] and information storage devices,[6] *etc.* Most of the ESPT reactions take place in molecules containing a vicinal proton donor and acceptor, *i.e.* intramolecular ESPT.[1c] If a molecule only has a proton donor (without an acceptor), or the proton donor is positioned too far from the acceptor, the ESPT reactions cannot spontaneously occur within the molecule and may occur between two such molecules or from one molecule to adjacent molecules, such as solvent molecules, *i.e.* intermolecular ESPT.[1b,7] The intermolecular ESPT process has also been found in biological systems, such as green fluorescence proteins and luciferin.[8] Compared with many molecules with intramolecular ESPT properties,[9] many fewer molecules showing intermolecular ESPT properties have been reported.[7,10] The reported intramolecular ESPT chromophores are limited to the structures of naphthols,[11] phenols,[7a,8a–c,8e,8f,10a,12] hydroxyquinolinuims,[13] *etc.* Because of the great potential of intermolecular ESPT processes in biological research and fluorescent probe design,[1c,14] the discovery of new chromophores with intermolecular ESPT properties is necessary.

Guanidines are the strongest organic bases (pK_a = 13.5) due to the resonance stabilization of their conjugated acids.[15] The guanidinium cation is very stable in aqueous solution over a wide pH range. Because the guanidinium group is capable of forming both electrostatic and hydrogen bond interactions with polar and anionic molecules,[15] guanidine derivatives have been used successfully as therapeutic agents,[16] DNA intercalating agents,[17] ligands for ion recognition,[18] and catalysts in organic synthesis.[19] 4-Amino-1,8-naphthalimides have been widely used as fluorescent and colorimetric sensors because of their advantageous optical properties, such as strong absorption and emission in the visible region, high photostability, large Stokes shift, and insensitivity to pH. These optical properties are due to the ICT process that is caused by "push–pull" substituent pairs (electron donor–acceptor pairs).[20]

In the research on sensor design, we observed a dual fluorescence emission phenomenon from a guanidine substituted naphthalimide, *N*-hydroxyethyl-4-guanidino-1,8-naphthalimide (ENG). This phenomenon has been rarely reported in the

[a]Beijing National Laboratory for Molecular Sciences, Key Laboratory of Analytical Chemistry for Living Biosystems, Institute of Chemistry, Chinese Academy of Sciences, Beijing, 100190, P.R. China. E-mail: sgdh@iccas.ac.cn; Fax: +86 10 62528509

[b]State Key Laboratory for Structural Chemistry of Unstable and Stable Species, Institute of Chemistry, Chinese Academy of Sciences, Beijing, 100190, China

[c]University of Chinese Academy of Sciences, Beijing 100049, China

† Electronic supplementary information (ESI) available. See DOI: 10.1039/c3tc30853g

studies of naphthalimides and guanidine derivatives.[17] In this paper, we measured the optical behaviors of the guanidine substituted naphthalimide, including steady-state spectra and time-resolved fluorescence, and investigated the pH-dependent spectral response, and the solvent effect on the spectral behaviors. The guanidine substituted naphthalimide was identified to be a new fluorophore with intermolecular ESPT properties. The application of ENG for F^- recognition was also investigated.

Results and discussion

The synthesis of guanidine substituted naphthalimides was carried out by the substitution reaction of 4-bromine-1,8-naphthalimides with guanidine (Scheme 1). Two compounds, *N*-hydroxyethyl-4-guanidino-1,8-naphthalimide (ENG) and *N*-butyl-4-guanidino-1,8-naphthalimide (TNG) were prepared for investigation.

The emission spectrum of ENG in acidic buffer (Fig. 1a) showed two emission bands with maxima at 470 nm and 580 nm, but the excitation spectra recorded at 470 nm and 580 nm only exhibited a single excitation band with a maximum at 350 nm, which suggests that two excited-state species occurred after the excitation of the ground-state ENG. Interestingly, the emission spectrum of ENG at pH 10.32 only shows a single emission band with a maximum at 580 nm, and the excitation spectrum recorded at 580 nm shows a red shifted band with a maximum at 400 nm (Fig. 1b). In order to understand the pH response mechanism of the ENG, the pH-dependent absorption spectra and emission spectra were investigated.

As shown in Fig. 2a, with the pH increasing from 3.59 to 11.32, the absorption band with a maximum at 350 nm decreased gradually, while a red shifted band with a maximum at 400 nm appeared and increased. The color of the solution was observed to change from colorless to yellow. The changes of both absorption bands showed a linear pH response in the range 6.5–10.5. The isoabsorptive point at 365 nm indicates that two distinct chromophores (acidic and basic forms of ENG) were present at the equilibrium. Therefore, the absorptions at 350 nm and 400 nm could be considered as the contributions of the acidic form (NGH^+) and basic form (NG) of ENG, respectively. The ground-state pK_a value of ENG was calculated to be 8.53 ± 0.03 based on the data of the absorbance change with pH at 350 nm (See ESI, Fig. S1†). This pK_a value can be assigned to the deprotonation of the guanidinium group of ENG. Although guanidine has a pK_a of 13.5 in water, the naphthyl substitution on the guanidine can greatly lower its pK_a,[21] and the electron-withdrawing imide moiety of naphthalimide is expected to further enhance the acidity of the guanidinium group. The large red shift of the absorption spectra of ENG in basic buffer is due to the electron-rich neutral guanidine group (deprotonated guanidinium), which causes a significant increase in the push–pull effect of the ICT transition of naphthalimide. This electron transfer effect can be proved by the considerable upfield shift of the ^1H NMR signals from the aromatic protons of the deprotonated form of ENG (Fig. S2†).

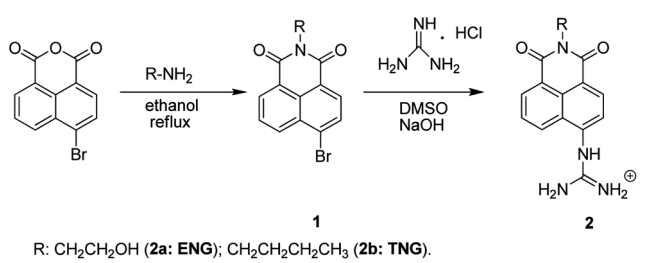

1 2

R: CH_2CH_2OH (**2a: ENG**); $CH_2CH_2CH_2CH_3$ (**2b: TNG**).

Scheme 1 Synthetic route of guanidine substituted naphthalimides.

The emission spectra of ENG (Fig. 2b) excited at the isoabsorptive point (365 nm) showed two emission bands (with maxima at 470 and 580 nm) at acidic pH; the emission band at 470 nm decreased gradually with an increase of the pH and showed a linear pH response in the range 6.5–10.0. However the emission band at 580 nm did not show significant change upon the pH increasing. At pH of above 10, the emission spectrum only showed the band with a maximum at 580 nm, and the absorption spectrum only showed the deprotonated NG band (with a maximum at 400 nm), suggesting that the band at 580 nm is the emission from the exited-state NG (NG*). Therefore the emission band at 470 nm (Fig. 1a, 2b and d) can be assigned to the emission from the excited-state NGH^+ (NGH^+*). The large Stokes shifts of the NGH^+* emission (120 nm) and NG* emission (180 nm) can be attributed to the efficient excited-state ICT process. However, at pH lower than 6.0, the emission spectrum of ENG also showed both NG* and NGH^+* bands, but the absorption and excitation spectra only showed the NGH^+ band (350 nm), and the Stokes shift of the NG* emission band was up to 230 nm. This phenomenon suggests that an excited-state deprotonation process (*i.e.* intermolecular ESPT from ENG to solvent) coupled ICT process occurred. As far as we know, this is the first report of a guanidinium group associated with an ESPT process.

The fluorescence spectra of ENG remained almost unchanged within the pH range from 3.0–6.5, because almost all the ENG was present in the NGH^+ form. But in the more acidic buffer, both emission bands changed with pH. As shown in Fig. 2c and d, the NG* band (580 nm) greatly decreased and the NGH^+* band (470 nm) slightly increased as the pH dropped from 3.38 to 0.3, while the absorption spectrum did not change. This set of results suggests that the ESPT process was inhibited in the more acidic solution. The excited state pK_a value (pK_a*) of ENG was calculated to be 0.895 ± 0.03 based on the fluorescence change with pH at 580 nm (Fig. S1†).

In order to exclude the possibility that the ESPT resulted from the hydroxyl proton of ENG, we synthesized *N*-butyl-4-guanidino-1,8-naphthalimide (TNG), an analogue of ENG without the hydroxyl group (Scheme 1). TNG showed almost identical optical properties to ENG in buffers with different pH values and various solvents (Fig. S3 and S4†). The pK_a and pK_a* of TNG were determined to be 8.49 ± 0.1 and 0.904 ± 0.08. These results suggest that the optical response to pH and the ESPT properties of ENG and TNG only relied on the moiety of guanidine substituted naphthalimide, and the substituents on the imide N-atom do not significantly affect these properties.

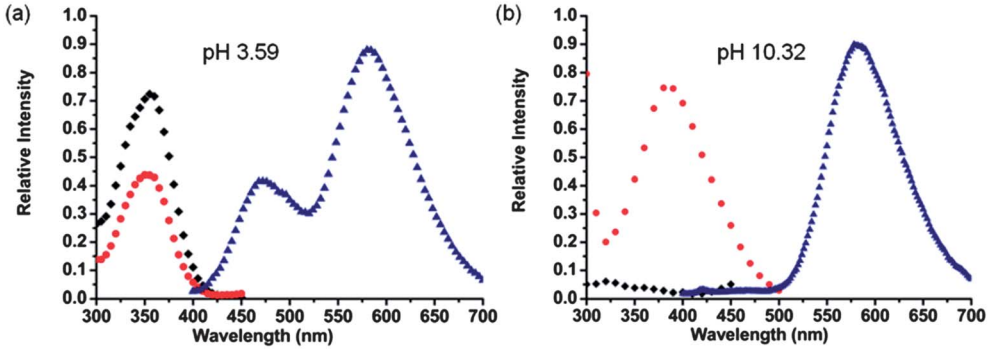

Fig. 1 Steady-state spectra of ENG were measured in glycine–HCl–NaOH buffer at pH (a) 3.59 and (b) 10.32; fluorescence spectra with excitation at 365 nm (up triangles), excitation spectrum detected at 460 nm (diamonds) and excitation spectra detected at 600 nm (circles).

The low pK_a* values of ENG and TNG indicate that the guanidine substituted naphthalimides can be considered as a new class of strong photoacid.

The excited-state deprotonation process of ENG can be illustrated as shown in Scheme 2. In neutral and acidic solution, most ENG molecules were present in the protonated form (NGH^+), upon excitation at 350 nm, some excited molecules in the protonated form (NGH^+*) quickly converted into the excited deprotonated form (NG*) through the intermolecular ESPT process. The NG* molecules returned to the ground state (NG) by emission with a band maximum around 580 nm. After returning to the ground state, the NG molecules reverted to the protonated form (NGH^+) *via* reverse proton transfer.

In order to further demonstrate the excited-state deprotonation process of ENG, time-resolved fluorescence spectroscopy of ENG in acidic buffer (pH 5.35), dichloromethane (DCM), dimethyl sulphoxide (DMSO) and ethanol were measured (Fig. 3). In these solvents, the NGH^+* emission showed an instant rise and an exponential decay, and the NG* emission showed an exponential rise followed by an exponential decay, which suggests the occurrence of an excited-state deprotonation process of ENG.[22] In polar solvents (acidic buffer, ethanol and DMSO), the rise time of NG* emission is comparable to the corresponding decay time of NGH^+* (Table 1), and both times are increased in the order of acidic buffer < ethanol < DMSO, which may suggest a decrease of the deprotonation rate of NGH^+*. The decay time of

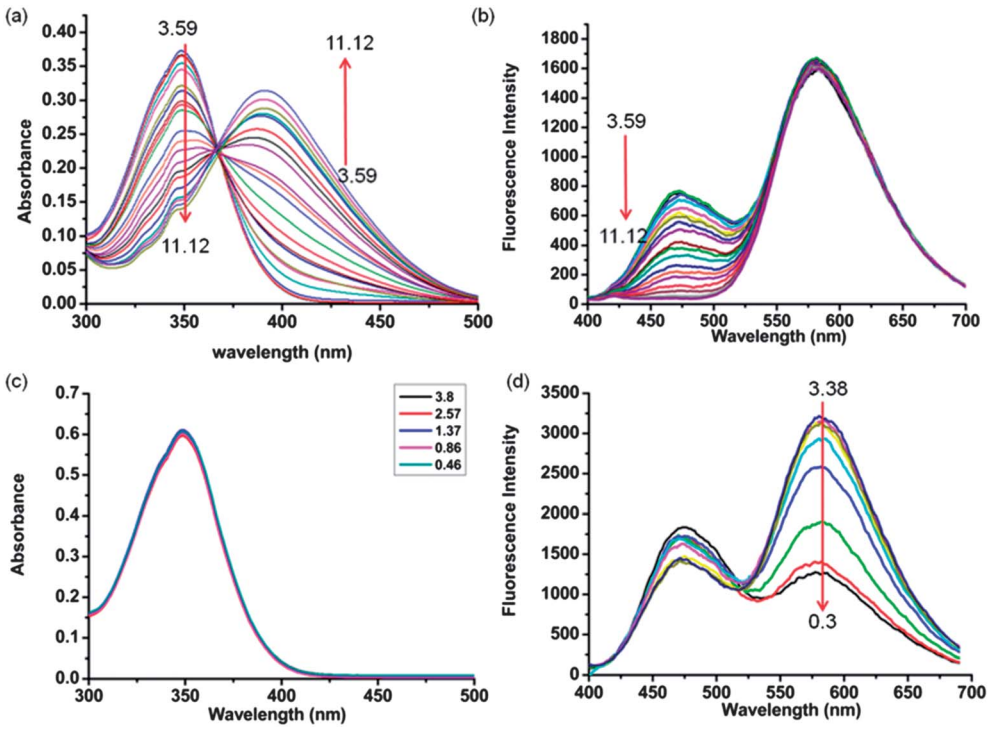

Fig. 2 (a) Absorption spectra of 30 μM ENG in glycine–HCl–NaOH buffer with pH 3.59, 5.52, 6.11, 7.3, 7.65, 7.82, 7.93, 8.05, 8.17, 8.32, 8.5, 8.62, 8.74, 8.94, 9.08, 9.21, 9.45, 9.71, 10.05, 10.32, 11.12; (b) fluorescence spectra of 30 μM ENG, excited at 365 nm; (c) absorption spectra of 50 μM ENG in glycine–HCl buffer at pH 3.8, 2.57, 1.37, 0.86, 0.46; (d) fluorescence spectra of 50 μM ENG in glycine–HCl buffer at pH 0.3, 0.39, 0.77, 1.11, 1.39, 1.79, 2.33, 2.62, 3.38, excited at 350 nm.

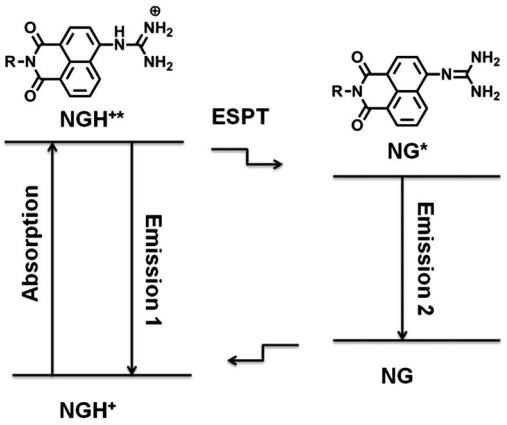

Scheme 2 Proton transfer reaction between the protonated form and deprotonated form of guanidine substituted 1,8-naphthalimides.

NG* emission increased in the same order, which is also consistent with the increase of the quantum yield (Φ_f) of ENG in these solvents (Table 2), suggesting the reduction of nonradiative rates of ENG. However, in dichloromethane, the rise time of NG* emission (1.57 ± 0.26 ns) is similar to that in DMSO, but is much faster than the decay of the NGH^+* emission (4.80 ± 0.06 ns), which may be due to the fact that only some of the NGH^+* molecules can undergo the deprotonation process. The slow decay of NGH^+* emission in dichloromethane suggests the significant suppression of the deprotonation process and the nonradiative decay of NGH* form.

Since the efficiency of ESPT reaction, especially the intermolecular ESPT is strongly dependent on the environment,[23] the solvent effect on the steady-state spectral properties of ENG was also investigated. As shown in Fig. 4a and b, in toluene, a low concentration of ENG (1 μM) only exhibited the NGH^+* emission peak (450 nm). When the concentration of ENG was increased, the NG* peak appeared and became stronger. Both emission bands were red-shifted with the increase of ENG concentration in toluene. This set of results suggests that the ESPT process could not occur from ENG to toluene. The NG* emission and the red-shifted emissions at high concentration of ENG may originate from the intermolecular interaction between two ENG molecules. As shown in Fig. 4c and d, ENG (1 μM) exhibited a high NGH^+* emission peak (450 nm) and a low NG* emission peak (530 nm) in dichloromethane. The NG* peak red shifted to 545 nm and became stronger than the NGH^+* peak in dioxane.

As summarized in Table 2, both emission peaks of ENG were red shifted as the solvent polarity was increased, but the absorption peak of ENG did not show significant shift in different solvents. Since 4-amino-1,8-naphthalimide is a typical fluorophore with ICT nature,[20] these results suggest that increasing solvent polarity stabilizes the ICT excited-state of both forms (NGH^+* and NG*) of ENG relative to the ground state and further lowers the energy of the excited-states. The fluorescence quantum yield of ENG decreased upon increasing the solvent polarity, and markedly decreased in a protic solvent, which is attributed to the increase in nonradiative decay

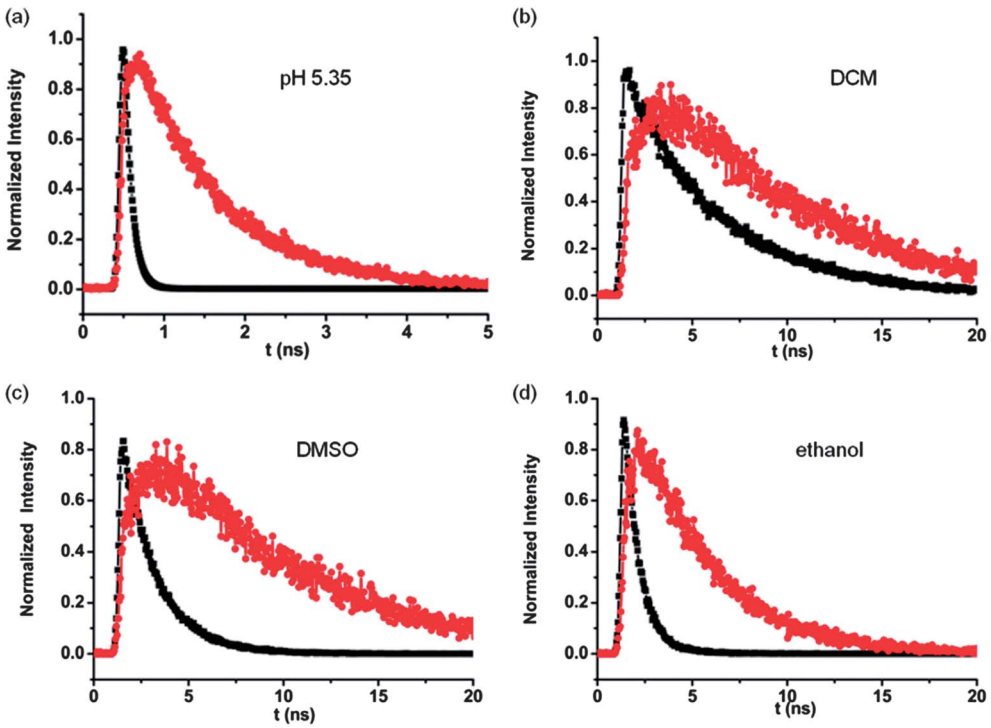

Fig. 3 The fluorescence dynamics of ENG (excitation at 350 nm) in (a) glycine–HCl–NaOH buffer with pH 5.35, emission: 460 and 560 nm; (b) DCM (dichloromethane), emission: 460 and 560 nm; (c) DMSO, emission: 460 and 560 nm; (d) ethanol, emission: 500 and 600 nm. Black curve, NGH^+* emission at 460 or 500 nm; red curve, NG* emission at 560 or 600 nm.

Table 1 Summary of time resolved fluorescence data of ENG in different solvents

Solvent	NGH^{+}* decay ns^{-1}	NG* increase ns^{-1}	NG* decay ns^{-1}
Buffer (pH 5.35)	0.09 ± 0.59	0.11 ± 0.02	1.03 ± 0.02
DCM	4.80 ± 0.06	1.57 ± 0.26	7.55 ± 0.57
DMSO	1.78 ± 0.01	1.47 ± 0.02	7.57 ± 0.05
Ethanol	0.81 ± 0.01	0.57 ± 0.08	3.81 ± 0.14

induced by the interactions between the ICT excited-state molecules and solvent molecules. (*e.g.* hydrogen bonding between the carbonyl oxygen and protic solvent)[24] The rapid nonradiative decay in a polar solvent is also demonstrated by the short lifetime of the both emissions (Fig. 3).

The ratio of the fluorescence intensity of NG* and NGH^{+}* changed in different solvents (Table 2). Surprisingly, in a polar solvent, acetonitrile, the NG* emission of ENG was very weak compared with the NGH^{+}* emission, suggesting that the ESPT from ENG to acetonitrile was unfavourable. In water, ENG exhibited the lowest quantum yield (0.018) and the fastest fluorescence decay (Fig. 3), but the ratio of the fluorescence intensity of NG* and NGH^{+}* was very high (1.70). In order to explain this phenomenon, the emission spectra of ENG were collected in DMSO or acetonitrile solution containing different amounts of water. As shown in Fig. 5a and b, both the NGH^{+}* and NG* emissions decreased significantly upon increasing the water in both solvents, but the decrease of the NGH^{+}* emission was much larger than that of the NG* emission, which caused the low quantum yield and high ratio of NG* and NGH^{+}* emissions in water. Obviously, there are many hydrogen-bonded sites in the ENG molecule, the multiple hydrogen-bonding interactions with water molecules cause the rapid nonradiative decay of the NGH^{+}* and NG* forms. Compared to the neutral NG* form, the hydration interaction of the cation NGH^{+}* further enhances the rapid nonradiative decay of NGH^{+}*, as well as the rapid deprotonation. A large deuterium isotope effect[25] on the quantum yields and the ratio of NGH^{+}* and NG* emission was also observed in D_2O (Table 2) relative to H_2O.

The emission behaviour of ESPT molecules in micelles was found to be markedly different to that in aqueous solution.[27] We further investigated the absorption and emission spectra in solution of surfactants like cetyl trimethylammonium bromide (CTAB), Triton X-100 and sodium dodecyl sulfate (SDS). The absorption spectra of ENG only showed a 350 nm band in these solutions, and did not show a notable change with the variation of surfactant concentration (Fig. S5†), suggesting that ENG was mainly present in the protonated form. As shown in Fig. 5c and d, both emission bands of ENG were not affected by CTAB and Triton X-100, but were greatly enhanced with an increase of the SDS concentration and reached a plateau near the critical micelle concentration (SDS, CMC 8 mM). Compared with in water, both emission bands of ENG in SDS solution were blue-shifted. These results suggest that the protonated ENG did not bind to cationic (CTAB, CMC 0.89 mM) and neutral (Triton X-100, CMC 0.2 mM) micelles, and strongly bound to anionic SDS even before its CMC. The binding to SDS provided a less polar microenvironment for ENG, and reduced the nonradiative decay by lowering the accessibility to bulk water.

The above results demonstrate that the emission properties of ENG can be tuned by changing its environment, which shows the potential application in versatile luminescent materials, such as white-light emitting materials.[4a,14] For this application, different color luminescence from blue to red was observed from ENG in different solvents (see Fig. S6†).

Recently, anion recognition and sensing have attracted considerable interest, because anions play important roles in the environment and in biological systems.[28] Guanidinium groups are extensively applied in anion recognition.[21] Fluorine

Table 2 Spectral properties of ENG in different solvents at room temperature (λ_{ex} = 350 nm)

Solvent	λ_{abs} (nm)	λ_{em} (nm) (NGH^{+a})	λ_{em} (nm) (NG^{a})	${I_{NG}}^{a}/{I_{NGH}}^{+a}$	${\Phi_f}^{a}$
Toluene (2 μM)	355	450	—	—	0.11
CH_2Cl_2 (2 μM)	350	448	530	0.75	0.29
$CHCl_3$ (2 μM)	345	450	535	1.38	0.32
Acetic ether (2 μM)	345	457	548	1.47	0.27
Dioxane (2 μM)	345	455	538	1.54	0.26
Acetone (2 μM)	345	452	551	1.83	0.24
Acetonitrile (2 μM)	345	445	—	—	0.21
DMF (2 μM)	345	462	564	0.43	0.22
DMSO (2 μM)	345	469	567	0.57	0.13
Ethanol (5 μM)	345	460	576	0.53	0.05
Methanol (5 μM)	345	467	570	0.35	0.06
H_2O (5 μM)	345	475	581	1.70	0.018
D_2O (5 μM)	345	472	582	1.33	0.038

[a] Quinine sulfate (Φ_f = 0.56) in 1.0 N sulfuric acid as standard.[26]

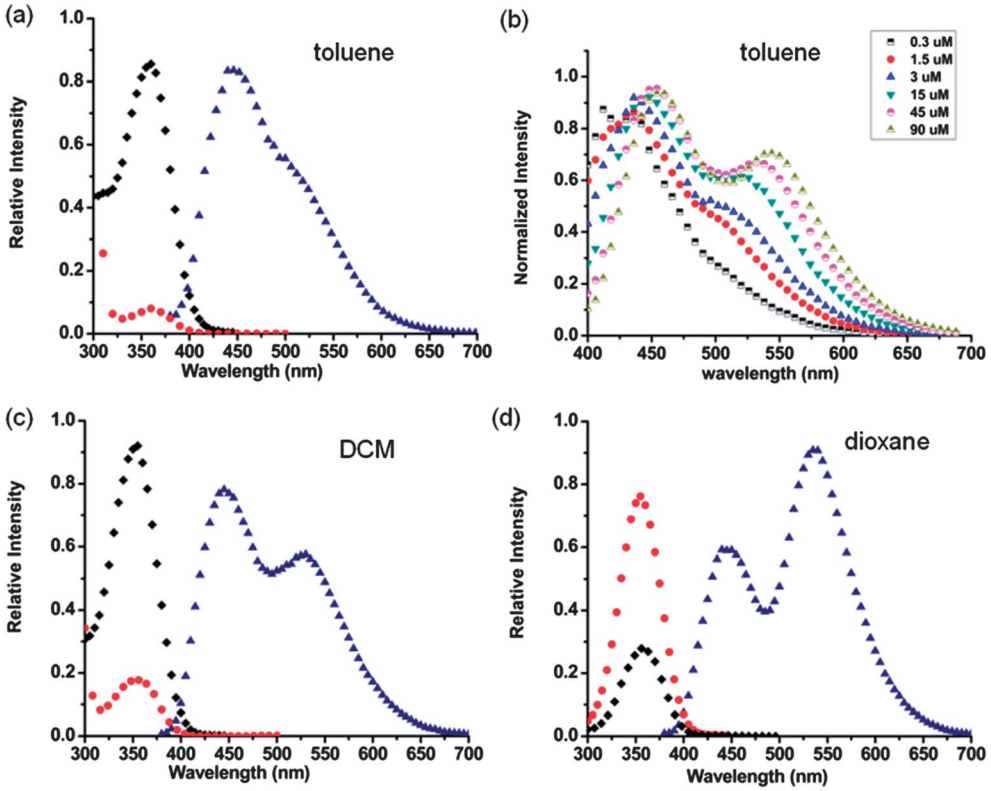

Fig. 4 Static excitation and fluorescence spectra of ENG in different solvents: (a) toluene (1 μM), (c) DCM (dichloromethane, 1 μM), and (d) dioxane (1 μM); fluorescence spectrum excited at 350 nm (up triangles), excitation spectrum detected at 460 nm (diamonds) and excitation spectrum detected at 600 nm (circles). (b) Fluorescence spectra of different concentrations of ENG (λ_{ex} = 350 nm) in toluene: 0.3 μM, 1.5 μM, 3 μM, 15 μM, 45 μM, 90 μM.

is the most electronegative atom, the anion of which usually forms the strongest H-bond interaction with an NH or OH group of an artificial receptor. Several receptors of F^- have been reported under the proton transfer signaling mechanism.[29] Therefore the interaction of ENG with F^- in acetonitrile and acetic ether was investigated by absorption and emission spectroscopy. As shown in Fig. 6a and c, upon the addition of F^- to ENG solutions (acetic ether or acetonitrile), the absorption band of ENG around 345 nm gradually decreased, while a band around 410 nm appeared and increased. An isosbestic point near 375 nm was observed. At the same time, the color of the ENG solution changed from colorless to yellow. Based on the above results, the two absorption bands can be assigned to the NGH^+ and NG forms of ENG. The change in the absorption spectra suggests that F^- induced the deprotonation of ENG in the ground state.

Although the emission spectra of ENG (excitation at isosbestic point) in acetic ether and acetonitrile were totally different in the absence of F^-, they showed a similar change upon the addition of F^-, *i.e.* the NGH^+* emission gradually decreased and the NG* emission gradually increased (Fig. 6b and d). Because F^- induced the deprotonation of ENG in the ground state, the NGH^+* emission decreased with the addition of F^- in both solvents. In acetonitrile, ENG mainly showed NGH^+* (450 nm) emission in the absence of F^-, therefore the NG* emission in the presence of F^- originated from the excitation of the NG form (Fig. S7†). In acetic ether, ENG showed NGH^+* (457 nm) and NG* (548 nm) emission in the absence of F^-, the NG* emissions in the presence of a low concentration of F^- (<2 μM) originated from the excitation of the NG form and the ESPT from the NGH^+* form. As shown in Fig. 6b and d, the NG* emission in acetic ether was much higher than that in acetonitrile when all the ENG molecules in the NGH^+ form were converted into the NG form by F^-, suggesting that acetonitrile may suppress the NG* emission of ENG. This result may also explain the low ESPT efficiency of ENG in acetonitrile.

Other halide anions could not significantly change the absorption and emission spectra of ENG (see Fig. S8†), indicating that ENG has a high selectivity for F^- sensing. The linear or ratiometric responses of the absorption and emission spectra to F^- suggest that ENG is a potential chemosensor for the highly sensitive detection of F^- (see Fig. S9 and S10†). The apparent equilibrium dissociation constants between ENG and F^- in acetic ether and acetonitrile were calculated to be 0.45 ± 0.02 μM and 0.78 ± 0.07 μM based on the curve of the fluorescence change at 457 nm and 445 nm (Fig. S9 and S10†). Neither the absorbance nor emission spectra of ENG were changed upon the addition of F^- in aqueous solution, which may due to the fact that water molecules compete for F^- with ENG as water molecules have a stronger acidity than ENG.

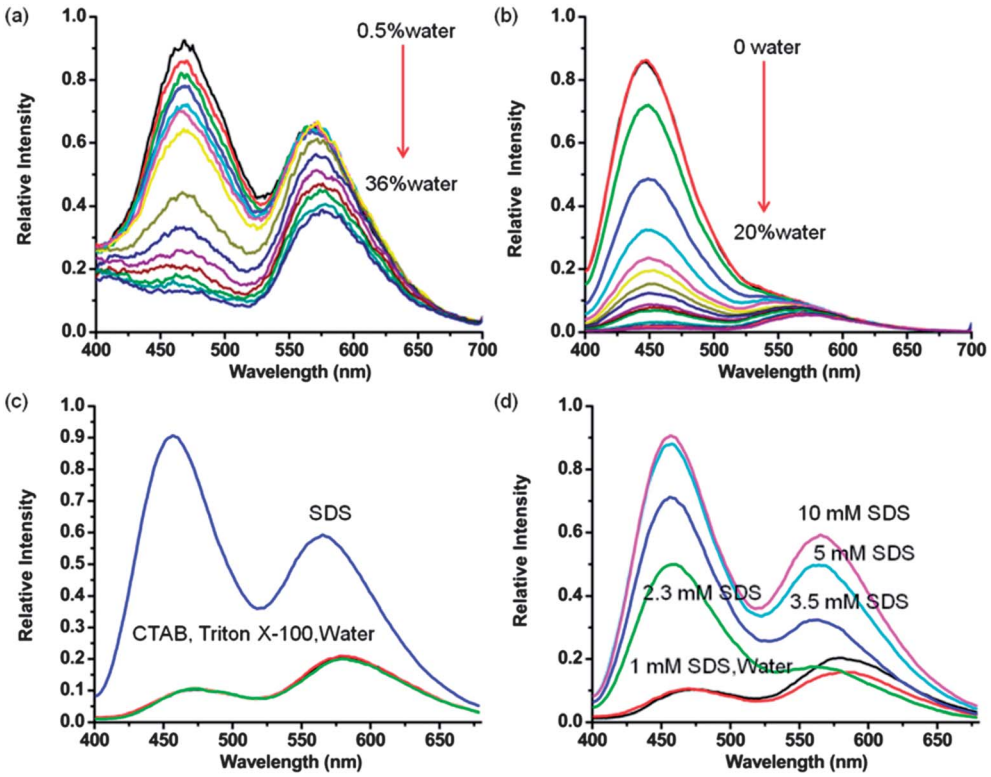

Fig. 5 Fluorescence spectra of ENG in solution containing different amounts of water, (a) H_2O/(DMSO + H_2O)%: 0.5, 1.0, 1.5, 2.0, 2.5, 3.0, 5.0, 10, 15, 20, 24, 28, 33, and 36; (b) H_2O/(CH_3CN + H_2O)%: 0.1, 0.5, 1.0, 1.5, 2.0, 2.5, 3.0, 3.5, 4.0, 4.5, 5.0, 5.5, 10, and 20; (c) steady-state emission spectra of ENG in water, 5 mM Triton X-100, 4 mM CTAB, 10 mM SDS; (d) steady-state emission spectra of ENG at different concentrations of SDS: 0 mM, 1 mM, 2.3 mM, 3.5 mM, 5 mM, 10 mM. $\lambda_{ex} = 350$ nm.

Conclusions

A new fluorophore based on guanidine substituted 1,8-naphthalimide was synthesized. The steady-state spectra and time-resolved fluorescence measurements demonstrated that the guanidinium group on this fluorophore possessed photoacidic properties with pK_a of ~8.5 and pK_a* of ~0.9. In acidic/neutral buffers or organic solvents, this fluorophore exhibits dual emission with large Stokes shifts in the wavelength range from 400–700 nm because of the ESPT coupled ICT process. This ESPT coupled ICT process is largely sensitive to the solvent microenvironment, implying the potential application in versatile luminescent materials. F^- can specifically induce the deprotonation of the guanidinium group of this fluorophore, resulting in a significant change in its absorption and emission spectra, suggesting the potential application as a chemosensor for F^-.

Experimental section

Chemicals

4-Bromo-1,8-naphthalic anhydride was purchased from Liao Yang Lian Gang Dye Chemical Co. Ltd (Liaoyang). Guanidinium hydrochloride was purchased from JK-chemical company (Beijing). Ethanolamine, ethanol, DMSO and other reagents were purchased from Beijing Chemical Plant (Beijing). Distilled-deionized water was used throughout this work. All chemical reagents were used without further purification. The stock solutions of ENG were obtained by dissolving it in DMSO. Tetrabutylammonium fluoride (TBAF), tetrabutylammonium chloride, tetrabutylammonium bromide, and tetrabutylammonium iodide were purchased from Acros and used without further purification. All stock solutions of anions and other molecules were dissolved in deionized water purified by a UPHW-III-90T Milli-Q water purification system (Chengdu, China). All of the titration experiments were performed at room temperature.

Instruments

^{1}H NMR spectra were recorded at 300 MHz, and ^{13}C NMR spectra were recorded at 75.5 MHz on a Brucker AM 300 spectrometer with tetramethylsilane (TMS) as the internal standard. *J* values were given in hertz. Low-resolution mass spectra (MS) were recorded on an LC-MS 2010A (Shimadzu) instrument using standard conditions. High-resolution MS were obtained on a Bruker Daltonics Flex-Analysis. UV-visible absorption spectra were recorded on a Hitachi U-2550 UV-vis spectrophotometer (Kyoto, Japan). Fluorescence emission spectra were recorded on a Hitachi F-4600 fluorescence spectrofluorometer (Kyoto, Japan).

The excitation laser pulses (350 nm) for the picosecond time resolved PL experiment were supplied by an optical parametric amplifier (OPA-800CF, Spectra Physics), which was pumped by the output from a regenerative amplifier (Spitfire, Spectra Physics). The excitation pulse energy was ~100 nJ per pulse. Fluorescence collected with a 90° geometry was dispersed by a

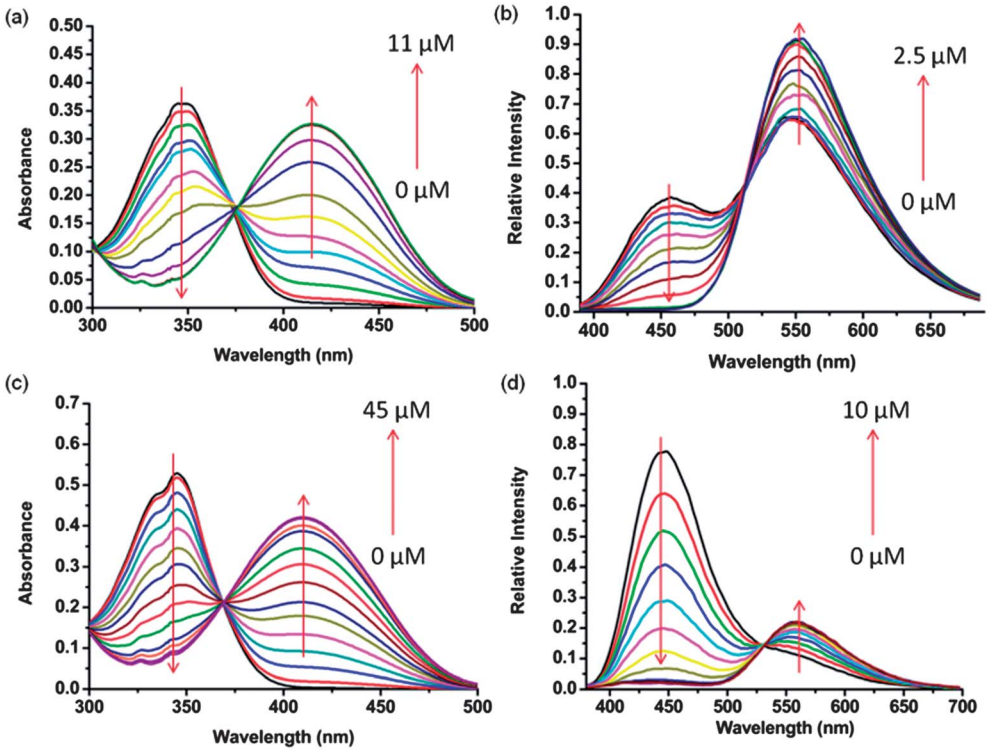

Fig. 6 (a) Absorption spectrum of ENG (40 μM) in acetic ether with different concentrations of F^- (TBAF in acetic ether solution): 0 μM, 1 μM, 2 μM, 3 μM, 4 μM, 5 μM, 6 μM, 7 μM, 8 μM, 9 μM, 10 μM, 11 μM; (b) fluorescence spectra of ENG (5 μM) in acetic ether with different concentrations of F^- (TBAF): 0 μM, 0.25 μM, 0.5 μM, 0.75 μM, 1.0 μM, 1.25 μM, 1.75 μM, 2.0 μM, 2.25 μM, 2.5 μM (excitation at 375 nm); (c) absorption spectra of ENG (40 μM) in acetonitrile with different concentrations of F^- (TBAF in acetonitrile solution): 0 μM, 3 μM, 5 μM, 7 μM, 11 μM, 15 μM, 19 μM, 23 μM, 27 μM, 31 μM, 37 μM, 41 μM, 45 μM; (d) fluorescence spectra of ENG (5 μM) in CH_3CN with different concentrations of F^- (TBAF): 0 μM, 1 μM, 2 μM, 3 μM, 4 μM, 5 μM, 6 μM, 7 μM, 8 μM, 9 μM, 10 μM (excitation at 365 nm).

polychromator (250is, Chromex) and detected with a photon-counting type streak camera (C5680, Hamamatsu Photonics). The spectral resolution was 0.2 nm, and the temporal resolution was ~50 ps. Analysis of the kinetic traces derived from time-resolved spectra was performed individually using nonlinear least-squares fitting to a general sum-of-exponentials function after deconvolution of the instrument response function (IRF). All the spectroscopic measurements were carried out at room temperature.

Spectral measurements

The absorption and fluorescence spectra were recorded in 20 mM glycine–HCl–NaOH buffer solution in a 1.0 cm quartz cuvette. Buffered solutions of different pH values were prepared by adding appropriate volumes of NaOH solution or HCl solution to the 20 mM glycine solution. A stock solution of ENG was prepared (10 mM) in DMSO. UV-vis absorption spectra and fluorescence spectra used the same concentration of solution made by adding 3 μL of stock solution to 1 mL of glycine–HCl–NaOH buffer solution.

Synthesis of *N*-hydroxyethyl-4-bromine-1,8-naphthalimide (ENA)

3.0 g (10.8 mmol) 4-bromine-1,8-naphthalic anhydride was dissolved in ethanol (160 mL), and heated to reflux. Then 730 μL of ethanolamine (11.9 mmol) was added to the mixture slowly. The resulting mixture was heated to reflux with stirring for 1 h. The reaction was over when the solution became clear. After the solution was cooled to room temperature, a precipitate emerged. A white solid was obtained by vacuum filtration, and then washed with water and ethanol three times each, and finally dried by vacuum (yield 93.2%);

^{1}H NMR ($CDCl_3$, 300 MHz) δ 8.65 (dd, $J = 7.5$ Hz, 1.5 Hz, 1H), 8.56 (dd, $J = 7.5$ Hz, 1.5 Hz, 1H), 8.40 (d, $J = 9$ Hz, 1H), 7.84 (dd, $J = 7.5$ Hz, 3 Hz, 1H), 4.42 (t, $J = 6$ Hz, 2H), 3.98 (t, $J = 6$ Hz, 2H), 2.09 (s, 1H); ^{13}C NMR ($CDCl_3$, 75.5 MHz) δ 162.9, 162.9, 132.5, 131.5, 131.3, 130.8, 129.7, 128.9, 128.7, 128.2, 122.8, 122.0, 57.7, 41.9; MS (ESI): m/z 320.1 $(M + H)^+$.

Synthesis of *N*-hydroxyethyl-4-guanidino-1,8-naphthalimide (ENG)

430 mg (1.3 mmol) *N*-hydroxyethyl-4-bromine-1,8-naphthalimide, 200 mg (2.1 mmol) guanidinium hydrochloride and 88 mg (2.2 mmol) NaOH were dissolved in DMSO (6 mL). The resulting mixture was heated to 80 °C for 12 h. After cooling to room temperature, the solution was evaporated under reduced pressure. The residue was purified by column chromatography using silica-gel (100–200 mesh) and 10% methanol in dichloromethane as eluent to give a yellow solid compound, then further purified by HPLC with chromatographic grade

methanol and 0.1% TFA in deionized water. A white solid compound was obtained (yield 29.7%).

^{1}H NMR (DMSO-d_6, 300 MHz) δ (ppm): 10.57 (s, 1N–H), 8.58 (d, $J = 6$ Hz, 1H), 8.54 (d, $J = 9$ Hz, 1H), 8.42 (d, $J = 9$ Hz, 1H), 7.97 (t, $J = 7.5$ Hz, 1H), 7.82 (d, $J = 9$ Hz, 1H), 7.79 (s, 4–NH–), 4.83 (t, $J = 12$ Hz, 1–OH), 4.18 (t, $J = 12$ Hz, 2H), 3.63 (t, $J = 6$ Hz, 2H); ^{13}C NMR (DMSO-d_6, 75 MHz) δ (ppm): 163.4, 163.0, 156.6, 137.6, 131.4, 131.2, 129.0, 128.6, 127.7, 127.4, 124.8, 122.6, 120.8, 57.7, 41.8. ^{1}H NMR (DMSO-d_6 + NaOH solid, 300 MHz) δ (ppm): 8.55 (d, $J = 6$ Hz, 1H), 8.45 (d, $J = 6$ Hz, 1H), 8.33 (d, $J = 9$ Hz, 1H), 7.72 (t, $J = 7.5$ Hz, 2H), 7.31 (d, $J = 6$ Hz, 1H), 6.56 (s, 4–NH–), 4.80 (s,1–OH), 4.15 (t, $J = 6$ Hz, 2H), 3.59 (t, $J = 6$ Hz, 2H); ^{13}C NMR (DMSO-d_6 + NaOH solid, 75 MHz) δ (ppm): 163.8, 163.1, 156.1, 132.5, 130.7, 130.6, 129.3, 127.4, 125.2, 121.9, 118.6, 113.3, 57.9, 41.5; MS (ESI): m/z 299.0 $(M + H)^+$; HRMS (ESI): m/z calcd for $C_{15}H_{15}N_4O_3$ $(M + H)^+$ 299.11387, found, 299.11356.

Synthesis of *N*-butyl-4-guanidino-1,8-naphthalimide (TNG)

2.5 g (9.03 mmol) 4-bromine-1,8-naphthalic anhydride was dissolved in 150 mL ethanol, and heated to reflux. Then 610 μL of butylamine (8.6 mmol) was added to the mixture slowly after the temperature was reduced to 50 °C. The resulting mixture was heated to reflux with stirring for 1 h. The reaction was over when the solution became clear. After the solution was cooled to room temperature, water was added to the solution and then a precipitate emerged. A white solid was obtained by vacuum filtration, and then washed with water and ethanol three times each, and finally dried by vacuum. *N*-Butyl-4-bromine-1,8-naphthalimide was obtained (yield 85.3%). Then 100 mg (0.302 mmol) *N*-butyl-4-bromine-1,8-naphthalimide, 78 mg (0.80 mmol) guanidinium hydrochloride and 44 mg (1.1 mmol) NaOH were dissolved in DMSO (4 mL). The resulting mixture was heated to reflux with stirring for 1 h. The resulting mixture was heated to 80 °C for 12 h. After cooling to room temperature, the solution was added to water and precipitation appeared in the solution. A brown solid was obtained by vacuum filtration. The residue was purified by column chromatography using silica-gel (100–200 mesh) and 5% methanol in dichloromethane as eluent to give a yellow solid compound, then further purified by HPLC with chromatographic grade methanol and 0.1% TFA in deionized water. A white solid compound was obtained (yield 33.5%).

^{1}H NMR (DMSO-d_6, 300 MHz) δ (ppm): 8.59–8.52 (m, 2H), 8.42 (d, $J = 6.0$ Hz, 1H), 7.97 (t, $J = 9.0$ Hz, 1H), 7.84 (s, 4–NH–), 7.82 (d, $J = 9.0$ Hz, 1H), 3.39 (t, $J = 6.0$ Hz, 2H), 1.67–1.60 (m, 2H), 1.39–1.31 (m, 2H), 0.93 (t, $J = 7.5$ Hz, 3H); ^{13}C NMR (DMSO-d_6, 75 MHz) δ (ppm): 163.2, 162.8, 156.7, 137.7, 131.4, 131.28, 129.0, 128.5, 127.28, 127.4, 124.8, 122.4.5, 120.7, 29.6, 19.7, 13.7; MS (ESI): m/z 311.2 $(M + H)^+$; HRMS (ESI): m/z calcd for $C_{15}H_{15}N_4O_3$ $(M + H)^+$ 311.15025, found, 311.1504.

Acknowledgements

We gratefully acknowledge the financial support from the grant 973 Program (2011CB935800 and 2013CB33700) and NSF of China (21075124 and 21275149).

Notes and references

1 (*a*) C. C. Hsieh, C. M. Jiang and P. T. Chou, *Acc. Chem. Res.*, 2010, **43**, 1364–1374; (*b*) T. Y. Lin, K. C. Tang, S. H. Yang, J. Y. Shen, Y. M. Cheng, H. A. Pan, Y. Chi and P. T. Chou, *J. Phys. Chem. A*, 2012, **116**, 4438–4444; (*c*) J. Wu, W. Liu, J. Ge, H. Zhang and P. Wang, *Chem. Soc. Rev.*, 2011, **40**, 3483–3495.

2 (*a*) K. Y. Chen, C. C. Hsieh, Y. M. Cheng, C. H. Lai and P. T. Chou, *Chem. Commun.*, 2006, **13**, 4395–4397; (*b*) M. D. McGehee and A. J. Heeger, *Adv. Mater.*, 2000, **12**, 1655–1668; (*c*) P. T. Chou, M. L. Martinez and J. H. Clements, *J. Phys. Chem.*, 1993, **97**, 2618–2622.

3 (*a*) D. Kuila, G. Kvakovszky, M. A. Murphy, R. Vicari, M. H. Rood, K. A. Fritch, J. R. Fritch, S. T. Wellinghoff and S. F. Timmons, *Chem. Mater.*, 1999, **11**, 109–116; (*b*) Y. P. Tsentalovich, O. A. Snytnikova, M. D. E. Forbes, E. I. Chernyak and S. V. Morozov, *Exp. Eye Res.*, 2006, **83**, 1439–1445.

4 (*a*) K. C. Tang, M. J. Chang, T. Y. Lin, H. A. Pan, T. C. Fang, K. Y. Chen, W. Y. Hung, Y. H. Hsu and P. T. Chou, *J. Am. Chem. Soc.*, 2011, **133**, 17738–17745; (*b*) S. Park, J. E. Kwon, S. H. Kim, J. Seo, K. Chung, S. Y. Park, D. J. Jang, B. M. Medina, J. Gierschner and S. Y. Park, *J. Am. Chem. Soc.*, 2009, **131**, 14043–14049; (*c*) J. E. Kwon and S. Y. Park, *Adv. Mater.*, 2011, **23**, 3615–3642.

5 E. S. Mansueto and C. A. Wight, *J. Am. Chem. Soc.*, 1989, **111**, 1900–1901.

6 M. Kamioka, Y. Ishikawa, H. Kaetsu, S. Isomura and S. Arai, *J. Phys. Chem.*, 1986, **90**, 5727–5730.

7 (*a*) N. Karton-Lifshin, I. Presiado, Y. Erez, R. Gepshtein, D. Shabat and D. Huppert, *J. Phys. Chem. A*, 2012, **116**, 85–92; (*b*) N. Alarcos Carmona, B. Cohen, J. Angel Organero and A. Douhal, *J. Photochem. Photobiol., A*, 2012, **234**, 3–11.

8 (*a*) Y. Erez and D. Huppert, *J. Phys. Chem. A*, 2010, **114**, 8075–8082; (*b*) Y. Erez, I. Presiado, R. Gepshtein and D. Huppert, *J. Phys. Chem. A*, 2011, **115**, 1617–1626; (*c*) I. Presiado, Y. Erez and D. Huppert, *J. Phys. Chem. A*, 2010, **114**, 13337–13346; (*d*) H. Hosoi, H. Mizuno, A. Miyawaki and T. Tahara, *J. Phys. Chem. B*, 2006, **110**, 22853–22860; (*e*) D. Stoner-Ma, A. A. Jaye, P. Matousek, M. Towrie, S. R. Meech and P. J. Tonge, *J. Am. Chem. Soc.*, 2005, **127**, 2864–2865; (*f*) N. Agmon, *Biophys.J.*, 2005, **88**, 2452–2461.

9 B. M. Uzhinov and M. N. Khimich, *Russ. Chem. Rev.*, 2011, **80**, 553–577.

10 (*a*) R. Daengngern, N. Kungwan, P. Wolschann, A. J. A. Aquino, H. Lischka and M. Barbatti, *J. Phys. Chem. A*, 2011, **115**, 14129–14136; (*b*) G. A. Brucker and D. F. Kelley, *J. Chem. Phys.*, 1989, **90**, 5243–5251.

11 (*a*) L. M. Tolbert and K. M. Solntsev, *Acc. Chem. Res.*, 2002, **35**, 19–27; (*b*) M. Lawrence, C. J. Marzzacco, C. Morton, C. Schwab and A. M. Halpern, *J. Phys. Chem.*, 1991, **95**, 10294–10299.

12 I. Presiado, Y. Erez and D. Huppert, *J. Phys. Chem. A*, 2010, **114**, 9471–9479.

13 E. A. Gould, A. V. Popov, L. M. Tolbert, I. Presiado, Y. Erez, D. Huppert and K. M. Solntsev, *Phys. Chem. Chem. Phys.*, 2012, **14**, 8964–8973.

14 J. Zhao, S. Ji, Y. Chen, H. Guo and P. Yang, *Phys. Chem. Chem. Phys.*, 2012, **14**, 8803–8817.
15 S. Walker, L. Chen, Y. N. Hu, Y. Rew, D. W. Shin and D. L. Boger, *Chem. Rev.*, 2005, **105**, 449–475.
16 (*a*) S. Ekelund, P. Nygren and R. Larsson, *Biochem. Pharmacol.*, 2001, **61**, 1183–1193; (*b*) A. Andreani, M. Granaiola, A. Leoni, A. Locatelli, R. Morigi, M. Rambaldi, G. Lenaz, R. Fato, C. Bergamini and G. Farruggia, *J. Med. Chem.*, 2005, **48**, 3085–3089; (*c*) C. E. Stephens, F. Tanious, S. Kim, W. D. Wilson, W. A. Schell, J. R. Perfect, S. G. Franzblau and D. W. Boykin, *J. Med. Chem.*, 2001, **44**, 1741–1748.
17 (*a*) C. Bailly, R. K. Arafa, F. A. Tanious, W. Laine, C. Tardy, A. Lansiaux, P. Colson, D. W. Boykin and W. D. Wilson, *Biochemistry*, 2005, **44**, 1941–1952; (*b*) K. Ohara, M. Smietana, A. Restouin, S. Mollard, J.-P. Borg, Y. Collette and J.-J. Vasseur, *J. Med. Chem.*, 2007, **50**, 6465–6475.
18 (*a*) Y. Sun, C. Zhong, R. Gong, H. Mu and E. Fu, *J. Org. Chem.*, 2009, **74**, 7943–7946; (*b*) M. R. Ganjali, M. Hosseini, F. Aboufazeli, F. Faridbod, H. Goldooz and A. R. Badiei, *Luminescence*, 2012, **27**, 20–23.
19 (*a*) T. Ishikawa, *Chem. Pharm. Bull.*, 2010, **58**, 1555–1564; (*b*) H. Miyabe, K. Yoshida, V. K. Reddy and Y. Takemoto, *J. Org. Chem.*, 2009, **74**, 305–311.
20 (*a*) L. Duan, Y. Xu and X. Qian, *Chem. Commun.*, 2008, **47**, 39–6341; (*b*) X. Qian, Y. Xiao, Y. Xu, X. Guo, J. Qian and W. Zhu, *Chem. Commun.*, 2010, **46**, 6418–6436; (*c*) C. L. Fang, J. Zhou, X. J. Liu, Z. H. Cao and D. H. Shangguan, *Dalton Trans.*, 2011, **40**, 899–903; (*d*) J. Zhou, C. L. Fang, T. J. Chang, X. J. Liu and D. H. Shangguan, *J. Mater. Chem. B*, 2013, **1**, 661–667; (*e*) B. Zhu, X. Zhang, Y. Li, P. Wang, H. Zhang and X. Zhang, *Chem. Commun.*, 2010, **46**, 5710–5712; (*f*) B. Zhu, C. Gao, Y. Zhao, C. Liu, Y. Li, Q. Wei, Z. Ma, B. Du and X. Zhang, *Chem. Commun.*, 2011, **47**, 8656–8658.
21 K. A. Schug and W. Lindner, *Chem. Rev.*, 2005, **105**, 67–113.
22 G. J. Woolfe and P. J. Thistlethwaite, *J. Am. Chem. Soc.*, 1981, **103**, 6916–6923.
23 (*a*) J. Seo, S. Kim and S. Y. Park, *J. Am. Chem. Soc.*, 2004, **126**, 11154–11155; (*b*) P. T. Chou, W. S. Yu, Y. M. Cheng, S. C. Pu, Y. C. Yu, Y. C. Lin, C. H. Huang and C. T. Chen, *J. Phys. Chem. A*, 2004, **108**, 6487–6498; (*c*) T. C. Swinney and D. F. Kelley, *J. Chem. Phys.*, 1993, **99**, 211–221; (*d*) K. Das, D. S. English and J. W. Petrich, *J. Am. Chem. Soc.*, 1997, **119**, 2763–2764; (*e*) B. Kang, K. C. Ko, S.-Y. Park, D. J. Jang and J. Y. Lee, *Phys. Chem. Chem. Phys.*, 2011, **13**, 6332–6339.
24 (*a*) A. Morimoto, T. Yatsuhashi, T. Shimada, L. Biczok, D. A. Tryk and H. Inoue, *J. Phys. Chem. A*, 2001, **105**, 10488–10496; (*b*) C. C. Chang, J. F. Chu, H. H. Kuo, C. C. Kang, S. H. Lin and T. C. Chang, *J. Lumin.*, 2006, **119**, 84–90.
25 L. Stryer, *J. Am. Chem. Soc.*, 1966, **88**, 5708–5712.
26 J. N. Demas and G. A. Crosby, *J. Phys. Chem.*, 1971, **75**, 991–1024.
27 (*a*) D. Roy, R. Karmakar, S. K. Mondal, K. Sahu and K. Bhattacharyya, *Chem. Phys. Lett.*, 2004, **399**, 147–151; (*b*) D. Mandal, S. K. Pal and K. Bhattacharyya, *J. Phys. Chem. A*, 1998, **102**, 9710–9714.
28 (*a*) F. P. Schmidtchen, *Coord. Chem. Rev.*, 2006, **250**, 2918–2928; (*b*) R. Martinez-Manez and F. Sancenon, *Chem. Rev.*, 2003, **103**, 4419–4476.
29 (*a*) B. Liu and H. Tian, *J. Mater. Chem.*, 2005, **15**, 2681–2686; (*b*) M. Vazquez, L. Fabbrizzi, A. Taglietti, R. M. Pedrido, A. M. Gonzalez-Noya and M. R. Bermejo, *Angew. Chem., Int. Ed.*, 2004, **43**, 1962–1965; (*c*) X. Zhang, L. Guo, F. Y. Wu and Y. B. Jiang, *Org. Lett.*, 2003, **5**, 2667–2670; (*d*) Z. R. Grabowski, K. Rotkiewicz and W. Rettig, *Chem. Rev.*, 2003, **103**, 3899–4031; (*e*) X. Huang, Y. He, Z. Chen and C. Hu, *Chin. J. Chem.*, 2009, **27**, 1526–1530.

